Sys Rev Pharm 2024; 15(9): 290-301
A multifaceted review journal in the field of pharmacy
E-ISSN 0976-2779 P-ISSN 0975-8453/DOI: 10.31858/0975-8453.15.9.290-301

Research Article

Synthesis and Optimization of Ethylene Glycol-Based Biolubricant from Castor (*Ricinus communis*) Seed Oil

Mustapha Aliru*, Olajide Aliru, Afolabi Usman Oladayo

Department of Chemistry and Industrial Chemistry, Kwara State University, Malete, Ilorin, Nigeria

Article History: *Submitted: 03.09.2024* *Accepted: 19.09.2024* *Published: 26.09.2024*

ABSTRACT

This work focuses on synthesizing and optimizing an ethylene glycol-based biolubricant derived from castor *Ricinus communis* seed oil to address environmental concerns associated with conventional lubricants. The process involved the extraction of Castor Oil (CAO), followed by physicochemical analysis and a two-step transesterification, resulting in a biodegradable and non-toxic CAO based biolubricant. Response Surface Methodology (RSM) was employed using a Box-Behnken Design (BBD) to optimize the second esterification process. This study focused on investigating the effects of input variables temperature, mole ratio and reaction time on the yield of biolubricant. CAO is rich in unsaturated fatty acids, with ricinoleic acid being the predominant component. The optimization process utilized a quadratic statistical model, which effectively identified the optimal reaction conditions a temperature of 80°C, a reaction time of 90 minutes, a molar ratio of 3:1 and a fixed catalyst dosage of 1.0%. Analysis of Variance (ANOVA) and model fittings showed the quadratic regression polynomial model is effective in optimizing biolubricant yield. The predicted yield of 85.96% closely aligned with the experimental value of 86.23% demonstrating the effectiveness of the model. The synthesized CAO based biolubricant affirms its quality and potential for industrial applications by meeting the requirements of International Organization for Standardization (ISO) Viscosity Grades 32 (ISO VG 32) and 46 (ISO VG 46).

Keywords: Lube synthesis, Non-edible oil, Quality standard, Statistical model, Biolubricant

***Correspondence:** Mustapha Aliru, Department of Chemistry and Industrial Chemistry, Kwara State University, Malete, Ilorin, Nigeria, E-mail: aliru.mustapha@kwasu.edu.ng

INTRODUCTION

Lubricants play a pivotal role in various industries including aviation, automobiles and machinery, offering essential functionalities such as wear particle elimination, friction reduction, increased efficiency, uniform heat distribution and minimized energy loss. In 2017, global lubricant consumption reached 36.1 million tons, with Africa contributing 6% to this demand and exhibiting an annual growth rate of 1.6% (Attia NK, *et al*., 2020). The African lubricants market, as of 2021, stood at 1.29 billion liters, projected to achieve a Compound Annual Growth Rate (CAGR) of 4.13%, reaching 1.58 billion liters by 2026 (Africa automotive, 2023).

Traditional lubricants, comprising 1%-30% performance enhancing additives and 70%-99% base stock, predominantly derived from petroleum products, raise environmental concerns due to their high toxicity, poor biodegradability, waste generation and adverse impacts on soil and air quality (Benedicto E, *et al*., 2017; Rakkan T, *et al*., 2018). Moreover, their usage contributes to the depletion of finite petroleum reserves, raising uncertainties about future availability and supply (Mustapha AO, *et al*., 2023). In response to these environmental challenges, biolubricant from vegetable oils have emerged as promising alternatives (Heikal EK, *et al*., 2017), due to their biodegradability, non-toxicity, eco-friendliness, negligible environmental risk, superior lubricity, high flash point, viscosity indices, shear stability and humidity resistance (Rakkan T, *et al*., 2018). CAO, derived from the seeds of the fast-growing *Ricinus communis* plant, presents advantages such as rapid biodegradability, non-toxicity, eco-friendliness and superior lubricity owing to its unique physical properties (Patel VR, *et al*., 2016; Yeboah A, *et al*., 2020).

Despite the benefits offered by biolubricants, challenges persist, including feedstock reliability, poor low-temperature performance and low thermal oxidative stability (Rakkan T, *et al*., 2018). To address these concerns, researchers have explored the incorporation of chemical additives such as Zinc Dialkyl Dithio Phosphates (ZDDP), phosphorous and sulfur. However, this improvement comes at a cost, with biolubricants being 30%-40% more expensive than their petroleum counterparts (Attia NK, *et al*., 2020). Overcoming this cost barrier necessitates advancements in production processes, catalyst modifications, or the exploration of alternative chemical processes like transesterification, selective hydrogenation and epoxidation (Attia Nk, *et al*., 2020).

Transesterification, a preferred method for biolubricant production, involves the reaction of polyhydric alcohol with Fatty Acid Methyl Esters (FAME) derived from vegetable oil (*Figure 1*). This process, facilitated by base catalysts, acidic catalysts, or enzymes, has shown promise in producing biolubricants with desirable fluidity and improved temperature performance (Musa U, *et al*., 2015). Commonly used polyhydric alcohols in transesterification include ethylene glycol, trimethylolpropane, pentaerythritoland neopentylglycol. Ethylene glycol in particular stands out for its excellent branched structure and anti-freezing properties making it a desirable choice for biolubricant production.

To optimize the transesterification process for biolubricant production various factors and reaction conditions such as the molar ratio of vegetable oil to alcohol, catalyst type, temperature, reaction time and fatty acid content in the feedstock must be considered (Uppar R, *et al*., 2023). In this study, we focus on synthesizing ethylene glycol-based biolubricant from CAO and employ RSM to optimize the molar ratio, temperature and reaction time, in order to achieve a high biolubricant yield.

MATERIALS AND METHODS

Castor *Ricinus communis* sees were purchased from Sunny agro-allied store, Agricarea, Ilorin-East LGA, ilorin, Kwara state Nigeria. While chemicals such as methanol, potassium hydroxide, n-hexane, potassium iodide, Isopropyl Alcohol (IPA), dichloromethane, sodium thiosulphate, acetone, sulphuric acid, ethylene glycol, phenolphthalein indicator, starch and potassium hydrogen phthalate were obtained from Sigma-Aldrich, Teddington Middlesex (UK) and Cerrilliant Round Rock, TX, USA.

Extraction and pretreatment of crude castor oil

The Crude Castor Oil (CCAO) was extracted from the castor seed by cold solvent extraction method was reported by (Bekele BA, *et al*., 2018) The castor seed was dried and pulverized using an electric blender. It was then submerged in n-hexane in the ratio 7:3 n-hexane to seed ratio for 72 hours. The mixture was then sieved. The filtrate was collected and distilled using a distillation apparatus then the CCAO was collected and then pre-treated using direct esterification of the oil with methanol using sulphuric acid as catalyst to reduce the Free Fatty Acid (FFA) content of the oil (Mustapha AO, *et al*., 2021).

Transesterification

The synthesis of a biolubricant involves a double transesterification process as shown in *Figure 1*. The first step produces an intermediate product Castor Oil Methyl Ester (COME) and in the second stepthis methyl ester is used as a reactant to synthesize the Coconut Oil Bio Lubricant (COBL).

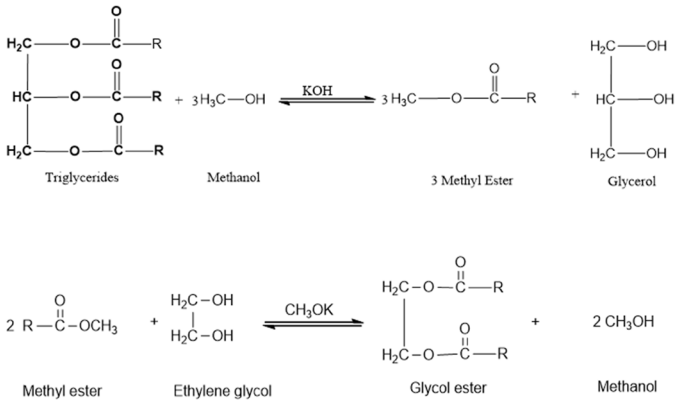

Figure 1: Equation of first and second transesterification reaction

Castor oil methyl ester synthesis

The synthesis of COME involves the reaction of the CAO with methanol using Potassium Hydroxide (KOH) as catalyst. A known amount of the pre-treated oil sample was weighted and placed in a two-neck round bottom flask equipped with a magnetic stirrer, refluxing condenser and a thermometer. A mixture of KOH at 1% w/v of the oil sample and methanol was added to the flask, was calculated in a ratio 1:6. The mixture was heated and stirred for 1 hour at 60°C-65°C. Then, the flask was removed from the hotplate and the reaction products were allowed to settle overnight resulting in two distinct liquid phases. The top phase ester was separated from bottom phase glycerol using a separating funnel and then washed for 3 times with warm water heated to 80°C to remove any excess catalyst until the wash water become clear. Finally, the ester phase was dried at 100°C for 30 minutes. The intermediate COME biodiesel was obtained as a clear liquid (Mustapha AO, *et al*., 2023).

Castor oil biolubricant synthesis

The COBL synthesis was carried out following the experimental design layout obtained from BBD. A known amount of COME to ethylene glycol were measured into a 250 mL of three-neck round bottom flask equipped with a magnetic stirrer, condenser and a thermometer. 0.8% of potassium methoxide was prepared by treating 0.3 g of KOH in 5 mL methanol and then heated for a few minutes. This was added to the reaction vessel as a catalyst. The reaction was conducted in a specific period of time at a particular temperature. The reaction was conducted under vacuum distillation conditions to ensure the complete removal of methanol produced from the reaction mixture. The percentage yield of biolubricant yield was then calculated using the equation below.

$$\%biolubricant\ yield = \frac{\text{weight of biolubricant produced}}{\text{weight of methylester}} \times 100$$

Optimization of biolubricant using response surface method

The relationships between independent variables methyl ester to ethylene glycol ratio, reaction time, temperature and response variable, percentage yield are established using the RSM for the transesterification of COME to biolubricant. RSM involves the use of a regression model that relies on a low-degree polynomial function along with ANOVA for each model to compute the p-value. A p-value of <0.05 for most process variables is considered favourable, indicating that the model terms are significant when the values are <0.0500. In this study, BBD was used to examine the input variables molar ratio, reaction time and temperature that influence biolubricant yield through the transesterification process was reported by (Ocholi O, *et al*., 2021). The factors or variables explored were assessed at three levels: Low level (-), medium level (0) and high level (+) as required by BBD. The experimental factor levels design is presented in *Table 1*.

Table 1: Factors levels of Input variables for biolubricant synthesis

Input variables	Notation	Unit	Low level (-)	Medium level (0)	High level (+)
Molar ratio	M	wt %	3:1	5:1	7:1
Temperature	θ	oC	60	80	100
Reaction time	T	Min	60	90	120

Design of Experiments (DOE)

The RSM must form a DOE with the minimum data to create accurate ANOVA models. BBD was used because it does not include axial points, ensuring that all design points fall within the operating limits. This requires fewer experimental runs. A BBD with three factors and three levels was adopted and the range of the variables affecting biolubricant yield is presented in *Table 1*. BBD specifies 17 experimental conditions to explore the effects of the three variables selected on biolubricant yield as shown in *Table 2*. These 17 experiments were accustomed to generate combinations that would help to determine the optimal conversion of biolubricant. After each experiment, the biolubricant yield was calculated and incorporated into the BBD for all the subsequent RSM investigations.

Table 2: Box-behnken design of experiments for biolubricant synthesis

Std.	Runs	Factor (A)	Factor (B)	Factor (C)	Molar Ratio (M)	Temp. (θ)	Time (T)
		M	θ	T	wt %	°C	Min.
15	1	0	0	0	5.1	80	90
7	2	-1	0	1	3.1	80	120
8	3	1	0	1	7.1	80	120
9	4	0	-1	-1	5.1	60	60
10	5	0	1	-1	5.1	100	60
12	6	0	1	1	5.1	100	120
2	7	1	-1	0	7.1	60	90
13	8	0	0	0	5.1	80	90
4	9	1	1	0	7.1	100	90
17	10	0	0	0	5.1	80	90
14	11	0	0	0	5.1	80	90
1	12	-1	-1	0	3.1	60	90
16	13	0	0	0	5.1	80	90
3	14	-1	1	0	3.1	100	90
11	15	0	-1	1	5.1	60	120
6	16	1	0	-1	7.1	80	60
5	17	-1	0	-1	3.1	80	60

The pure error and lack of fit were estimated using five center points for the proposed model (Betiku E, *et al*., 2016). A second-order polynomial equation was utilized to express the biolubricant synthesis (Y) as a function of the independent variables. The optimum percentage yield of the biolubricant predicted by the model was then experimentally validated in the laboratory and the experimental yield was compared against the predicted yield.

Characterization of castor oil, biodiesel and biolubricant

The fatty acid profile of the samples was determined using Gas Chromatography Mass Spectrometry (GC-MS) analysis. The physicochemical properties of the COME and CAO based biolubricant were determined using American Society for Test and Materials (ASTM) standard methods. The Fourier Transform Infrared Spectroscopy (FTIR) technique was used to investigate the synthesized biolubricant and identify its functional groups. The FTIR analysis confirmed the successful synthesis of both the methyl ester and the biolubricant. FTIR analysis was conducted using Shimadzu equipment. Lubricant properties of the synthesized CAO biolubricant, including Pour point, flash point, fire point and cloud point, were evaluated according to ASTM D6751-09 standards and Leevijit method (Leevijit T, *et al*., 2016).

RESULTS AND DISCUSSION

Properties of crude and refined CAO

The physicochemical properties of crude and pretreated CAO are presented in *Table 3*. These properties were compared with those of other oils in relation to the ASTM D6751-09 recommended standards. The CCAO appeared golden yellow at room temperature, similar in color to rubber seed oil (Reshad AS, *et al*., 2015), although it is slightly differed from ASTM standard. The yield of CCAO after extraction with n-hexane was 39.8% w/w. This relatively low yield may be attributed to the solubility of CAO in n-hexane, influenced by the polar nature of ricinoleic acid. This result is consistent with the findings reported by (Pradhan S, *et al*., 2021), who achieved a yield of 48% w/w yield using methyl alcohol and 38% w/w using n-hexane as solvents for the extraction process. The density of the CCAO was 0.90 g/cm^3, indicating that the oil is lighter than water but heavier compared to the results reported by (Heikal EK, *et al*., 2017) and this density falls within the ASTM standard range. The viscosity of CCAO at 40°C was found to be 98.03 cSt, which is lower than the value obtained by (Pradhan S, *et al*., 2021) but higher than the results reported by (Heikal EK, *et al*., 2017; Reshad AS, *et al*., 2015) The high viscosity of CCAO makes it suitable as biolubricant. There is a small difference between the density and viscosity of CCAO and Refined Castor Oil (RCAO). The acid value of CCAO was 8.42 mg KOH/g, with a FFA content of 4.23% which is high for transesterification reactions. To prevent excessive oil saponification during transesterification, it is necessary to reduce the FFA to 3.37 mg KOH/gand 1.69% respectively for RCAO. The efficiency of esterification (pretreatment) was determined to be 60.04%. The iodine value and saponification value of RCAO used in this study were 95.18 I2/100g and 180.96 mg/KOH, respectively. Saponification Value (SV) serves as an index of the average molecular mass of fatty acid in the oil sample. It measures oxidation during storage and indicates deterioration of the oils. The iodine value measures the degree of unsaturation in vegetable oil, while an increase in saponification value in oil is associated with increased. In this study, the saponification value obtained is slightly lower compared to the findings of (Pradhan S, *et al*., 2021) who reported a value of 186.00 mg/KOH for CAO and (Mokhtar SM, 2018), who reported 199.13 mg/KOH for *Jatropha* oil. The iodine value obtained in this study is higher than the results reported by (Pradhan S, *et al*., 2021; Reshad AS, *et al*., 2015) as well as the ASTM standard. This indicates that crude avocado oil has a high percentage of unsaturated fatty acids. Additionally, the low acid value and the high saponification value of CAO indicate that the trans esterified oil can be used as fuel.

Table 3: Physicochemical properties of castor oil compared with different seed oils

Physicochemical properties	Crude Castor Oil (CCAO)	Refined Crude Castor Oil (RCAO)	Castor oil[a]	*Jatropha curcas* L oil[b]	Rubber seed oil[c]	ASTM Standard D6751-09
Yield (% w/w)	39.80	80	38	39.50	-	-
Colour	Golden yellow	Golden yellow	-	-	Golden yellow	Amber
Specific gravity (g/cm^{-3}, 30°C)	0.94	0.93	0.96	-	-	0.957-0.968
Density at 30°C (g/cm^3)	0.90	0.89		0.86	0.91	0.88-0.95
Kinematic viscosity (Cst, 40°C)	98.03	84.52	240	77.4	30.00	50-60
Acid value (mg KOH/g)	8.42	3.37	0.92	4.65	12.12	0.40-4.00
Saponification value (mg/KOH)	186.56	180.96	186	199.13[d]	235.58	175-187
Iodine value (I^2/100g)	97.18	95.18	91.00	87.56	113.00	82-88
Ester value (mg KOH/g)	178.14	177.58	-	-	-	-
% Glycerine	9.71	-	-	-	-	-
% FFA	4.23	1.69	-	2.34	6.09	0.3-1.0
Average molecular weight (g/mol^{-1})	-	947.70	-	863.08[d]	-	-

Note: a: Castor oil; b: *Jatropha curcas* L. oil; c: Rubber seed oil

Fatty acid profile of CAO

Fatty acids profile of CAO was analyzed using GC-MS. The GC-MS chromatogram (*Figure 2*), revealed the presence of 9 fatty acids in the CAO sample, as detailed in *Table 4*. Among these, four saturated fatty acids and five are unsaturated fatty acids. The CAO contains several saturated fatty acids, including caprylic acid, lauric acid, palmitic acid and stearic acid. In contrast, the unsaturated fatty acids present in the CAO are petroselinic acid, linoleic acid, oleic acid, ricinoleic acid and eicosenoic acid. The results indicate a higher percentage of unsaturated fatty acids 84.75% compared to saturated fatty acid 15.25%. This significant proportion of unsaturated fatty acids indicates that the oil is a good source of these beneficial compounds, which is further supported by the high iodine value obtained for the CAO. Ricinoleic acid is the predominant fatty acid in CAO, accounting for 68.89% followed by linoleic acid at 15.21% and palmitic acid at 14.97%. Among the saturated fatty acids, palmitic acid has the highest percentage.

The fatty acid profile obtained in this study aligns with existing literature on CAO. (Guo S, *et al*., 2018) reported the presence of Ricinoleic acid (90.85%), Oleic acid (2.82%), Linoleic acid (3.74%), Stearic acid (0.64%) and Palmitic acid (0.72%). Similarly, (Pradhan S, *et al*., 2021) reported the presence of Ricinoleic acid (87.1%), Oleic acid (3.2%), Linoleic acid (5.1%), Stearic acid (1.51%), Linolenic acid (0.5%) and Palmitic acid (1.25%). Ricinoleic acid, a monounsaturated fatty acid is the dominant acid constituting about 75%-90% of the total oil composition. The results of this study showed a lower percentage of ricinoleic acid compared to existing literature; however, remains the highest fatty acid in the sample. The fatty acid profile of CAO indicates low amount of saturated and high unsaturated fatty acids, which enhances its stability (Yusuf AK, *et al*., 2015).

Properties of synthesized CAO methyl ester

The yield of the COME was found to be 94.76%. The high yield may be due to the increased forward reaction during the transesterification process, as well as the low level of FFA in CAO. The phytochemical properties of COME were determined and are reported in *Table 5*. (Silitonga AS, *et al*., 2020) reported the percentage yield of 95.42% yield for *Ceiba pentandra* methyl ester. The COME obtained has density of 0.78 g/cm^3 and viscosity of 4.39 cSt. These values are lower than those reported by (Singh D, *et al*., 2019; Binhweel F, *et al*., 2021) which were the value 0.88 g/cm^3 and 0.89 g/cm^3 respectively, indicating that the values do not meet ASTM standard. The acid value obtained in this study is higher compared to (Singh D, *et al*., 2019; Binhweel F, *et al*., 2021), but it aligns with the maximum ASTM standard value. Additionally, COME has a heating or calorific value of 50.63 MJ/kg which is higher than the ASTM standard.

The calorific value represents the thermal content of biodiesel released during combustion when biodiesel fuel is completely burned under controlled conditions (Sivaramakrishnan K and Ravikumar P, 2011). Thus, the heating value is another expression for the energy content of biodiesel. The level of unsaturation in biodiesel significantly influences its heating value, as unsaturated esters possess high volumetric energy and low mass energy (Binhweel F, *et al*., 2021). The high iodine value of the synthesized COME account for high level of unsaturation, which contributes to its high calorific value.

Fourier transform infra-red spectrometry analysis

The FTIR spectra of a) CAO, b) COME and c) COBL were shown in *Figure 3*. Several peaks were observed at the functional group region 4000 cm^{-1} to 1200 cm^{-1}. The peaks revealed in CAO are 1463.69 cm^{-1}, 1742.85 cm^{-1}, 2855.10 cm^{-1}, 2927.18 cm^{-1},3008.05 cm^{-1}and 3543.16 cm^{-1}. These peaks indicate the presence of various functional groups O-CH$_2$ glycerol group, C=O Ester carbonyl, C-H alkanes, C-H aliphatic, =C-H alkenes and O-H hydroxyl group respectively. The presence of the glycerol group and ester carbonyl functional group confirms the existence of a triglyceride backbone in CAO, while the C-H aliphatic, =C-H alkene and O-H hydroxyl groups indicate the fatty acid chain. The -OH group may be attributed to the hydroxyl group on the ricinoleic acid of CAO. Additionally, peak at 1019.74 cm^{-1} confirms the presence of an ester group C=O-CH$_3$ in the isolated molecule, while the C-H alkenes indicate the unsaturated fatty acid chain of the CAO (*Table 6*).

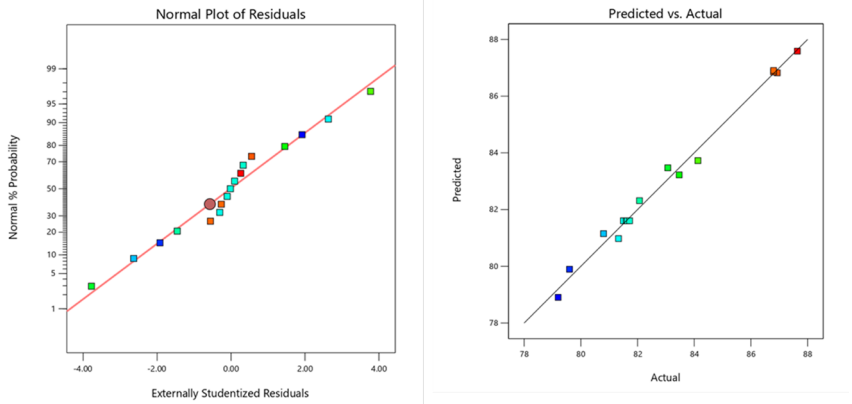

Figure 2: Normal plots of (a) residue and (b) predicted *vs*. actual value

Table 4: Fatty acid profile of castor oil

Saturated fatty acids		Unsaturated fatty acids	
Compound	**Relative abundance (%)**	**Compound**	**Relative abundance (%)**
Caprylic acid ($C_8H_{16}O_2$)	0.11	Petroselinic acid ($C_{18}H_{34}O_2$)	0.12
Palmitic acid ($C_{16}H_{32}O_2$)	14.97	Ricinoleic acid ($C_{18}H_{34}O_3$)	68.89
Lauric acid ($C_{12}H_{24}O_2$)	0.03	Linoleic acid ($C_{16}H_{32}O_2$)	15.21
Stearic acid ($C_{18}H_{36}O_2$)	0.15	Oleic acid ($C_{18}H_{34}O_2$)	0.44
-	-	Eicosenoic acid ($C_{20}H_{38}O_2$)	0.08
Total=15.25		Total=84.75	

Table 5: Physicochemical characteristics of castor oil methyl ester

Physicochemical properties	Castor Oil Methyl ester (COME)	*Jatropha* oil methyl ester[a]	Camelia oil methyl ester[b]	ASTM standard
Yield (%)	94.76%	-	-	-
Density at 30°C (g/cm^{-3})	0.78	0.88	0.89	0.85-0.90
Kinematic Viscosity (cSt,) at 40°C	4.39	4.80	4.53	1.9-6
Acid value (mg KOH/g)	0.89	0.48	0.35	0.8 max
Saponification value (mg/KOH)	242.68	-	-	-
Iodine value (I^2/100g)	126.90	95.75	146.5	-
Calorific value (MJ/kg)	50.63	40.79	52.2	37.3
Average molecular weight (g/mol^{-1})	698.34	221.61	-	-

Note: a: *Jatropha* oil methyl ester; b: Camelia oil methyl ester

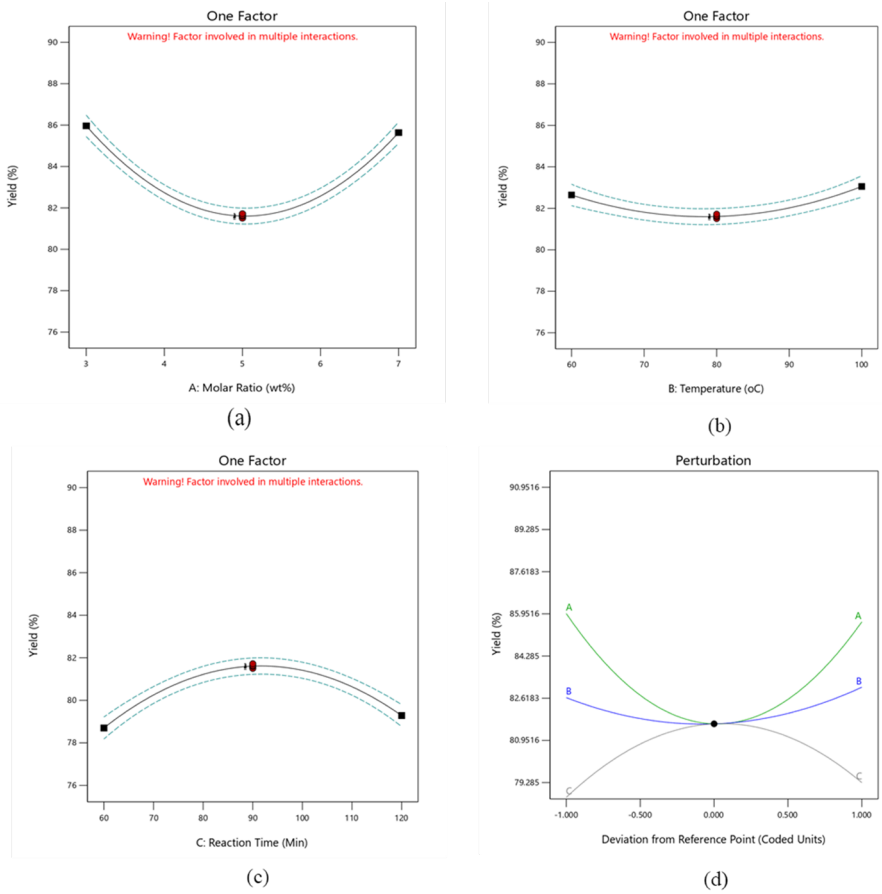

Figure 3: a): Effect of molar ratio on COBL yield at temperature 80°C and time 90 minutes; b): Effect of temperature on the COBL yield at molar ratio 5 and time 90 minutes; c): Effect of factor C, reaction time on the COBL yield at molar ratio 5 and temperature 80°C and d): Perturbation plot for the factors

Table 6: FTIR analysis of Castor Oil Methyl Ester (COME)

	O-CH_2 (Glycerol group)	C=O (Ester carbonyl)	C-H (Aliphatic)	C=O-CH_3 (Methyl ester group)	C=C-H (Stretch alkenes)	O-H (Alcohol)
CAO (cm^{-1})	1463.69	1742.85	2927.18	-	3008.05	3543.16
COME (cm^{-1})	-	1742.49	2927.22	1173.33	3008.51	3431.55
COBL (cm^{-1})	-	1742.37	2926.19	-	3008.32	3432.63

In contrast, COME showed peaks at 1173.33 cm^{-1}, 1653.07 cm^{-1}, 1742.49 cm^{-1}, 2855.18 cm^{-1}, 3008.51 cm^{-1} and 3431.55 cm^{-1} which indicates the presence of C=O-CH_3 ester group, C=C alkene, C=O ester carbonyl, C-H aliphatic, C-H alkene group and O-H alcohol respectively. The presence of the C=O ester at 1742.49 cm^{-1} and a strong C-H aliphatic peak, which was absent in CAO indicates the formation of a methyl ester as shown in *Figure 3*. The FTIR spectrum of COBL shows strong absorption bands at 1559.87 cm^{-1} and 1742.37 cm^{-1} corresponding to carbonyl C-O stretching and that of C=O at 1198.35 cm^{-1} due to asymmetric and symmetric axial stretching. The stretching vibrations of CH_3 and CH_2 appear at 2854.10 cm^{-1} and 2926.19 cm^{-1} respectively. The presence of ester group C-O and the absence of the CH_3-C=O ester group formed COME indicate complete transesterification and synthesis of COBL.

Optimization of CAO ethylene glycol ester (biolubricant) yield

BBD tool was used in the RSM to optimize the effect of process parameters, molar ratio (A), temperature (B) and time (C) on the yield of COBL (Mohammed IS, *et al*., 2019).

Experimental yield

The experimental yields of COBL synthesized according to the design of experiments are presented in *Table 7*. The results indicate that the COBL yield across all 17 experiments ranged from 79.20%-87.64%. The experiment with standard order 3 and run 14 with molar ratio 3, temperature of 100°C and reaction time of 90 minutes, has the highest yield of 87.64%. In contrast, the experiment with standard order 9 and run 4, which had a molar ratio of 5, a temperature 60°C and a reaction time of 60 minutes, yielded the lowest result at 79.20%.

Model fitting and analysis of variance

BBD evaluated various models for the experimental data, including linear, Two-Factor Interaction (2FI), quadratic and cubic models. The fit summary of these models is presented in *Table 8*. The quadratic model was selected as the best fit due it its low standard deviation, significant p-value<0.05, least significant lack of fit value which assesses the difference between pure and residual errors and high predicted and adjusted R^2 values. In contrast, the linear and 2FI models were eliminated because they have high standard deviations and p-value>0.5. Although the cubic model had an acceptable standard deviation, it was not chosen because it was marked as aliased, indicating that it contained aliased terms; further tests would be required to estimate all model terms independently.

The results of the ANOVA and the quadratic polynomial equation proposed by BBD confirmed that the selected quadratic model is the most suitable regression equation in mathematical modeling in estimating the yield of COBL synthesis. The quadratic polynomial equation is a second-order polynomial that represents COBL yield as a function of the three variables molar ratio (M), temperature (°C) and reaction time (min). The equation is presented below

$$Y = +94.21725 - 10.83563A - 0.339488B + 0.609225C - 0.004438AB + 0.006917AC - 0.001387BC + 1.04863A^2 + 0.003105B^2 - 0.002906C^2$$

Where Y is for COBL Yield, while A, B and C denote the molar ratio (M), temperature (°C) and time (min), respectively. The coefficients A, B and C reflect the direct linear impacts of these independent process variables. In contrast, the linear interaction effects between the variables are represented by AB molar ratio/temperature, AC molar ratio/time and BC temperature/time. The quadratic effects of the independent variables are A^2, B^2 and C^2.

The ANOVA table for the quadratic model related to COBL synthesis was shown in *Table 9* as proposed by BBD. The ANOVA analysis examines the relationship between the variables and assesses the importance of each model term. A p-value<0.05 indicates that a model term has a statistically significant impact on the response variable, while a p-value>0.1 suggests that the model term is not statistically significant. The ANOVA results for this study showed that the model terms BC, A^2, B^2 and C^2 are significant. Therefore, the temperature/time interactions and the independent variables molar ratio (M), temperature (°C) and time (min) have a significant impact on COBL yield.

Table 7: Experimental yields (%) of COBL synthesized using the experimental design

Std.	Runs	Molar Ratio (A)	Temp. (B)	Time (C)	Yield (Y)
		wt %	°C	Min.	%
15	1	5:1	80	90	81.60
7	2	3:1	80	120	83.47
8	3	7:1	80	120	84.13
9	4	5:1	60	60	79.20
10	5	5:1	100	60	81.33
12	6	5:1	100	120	79.60
2	7	7:1	60	90	86.80
13	8	5:1	80	90	81.57
4	9	7:1	100	90	86.80
17	10	5:1	80	90	81.72
14	11	5:1	80	90	81.50
1	12	3:1	60	90	86.93
16	13	5:1	80	90	81.64
3	14	3:1	100	90	87.64
11	15	5:1	60	120	80.80
6	16	7:1	80	60	82.07
5	17	3:1	80	60	83.07

Table 8: Fit summary for the optimization models

Source	Std. Dev.	Sequential p-value	Lack of fit p-value	Adjusted R^2	Predicted R^2	Remark
Linear	2.91	0.9853	<0.0001	-0.2172	-0.9938	Not suggested
2FI	3.27	0.9511	<0.0001	-0.5309	-3.5982	Not suggested
Quadratic	0.3627	<0.0001	0.0016	0.9811	0.8713	Suggested
Cubic	0.0817	0.0016	-	0.9990	-	Aliased

Table 9: Analysis of Variance (ANOVA) table for the quadratic model for COBL synthesis

Source	Sum of squares	df	Mean square	F-value	p-value
Model	110.60	9	12.29	93.41	<0.0001
A-Molar ratio	0.2145	1	0.2145	1.63	0.2423
B-Temperature	0.3362	1	0.3362	2.56	0.1539
C-Reaction time	0.6786	1	0.6786	5.16	0.0574
AB	0.1260	1	0.1260	0.9580	0.3603
AC	0.6889	1	0.6889	5.24	0.0559
BC	2.77	1	2.77	21.07	0.0025
A^2	74.08	1	74.08	563.10	<0.0001
B^2	6.50	1	6.50	49.37	0.0002
C^2	28.80	1	28.80	218.94	<0.0001
Residual	0.9209	7	0.1316	-	-
Lack of fit	0.8942	3	0.2981	44.62	0.0016
Pure error	0.0267	4	0.0067	-	-
Cor total	111.52	16	-	-	-

Type III-partial methods

The Model F-value of 93.41 implies that the model is significant, with only a 0.01% chance that an F-value this large could occur due to noise. The model's Coefficient of Variation (CV) and R^2 value were 0.4373 and 0.9917, respectively (*Table 10*). The CV is the ratio of the standard error of the estimate to the mean value, indicating the degree of precision with which the experiment was carried out. A low value of CV indicates high reliability and precision; however, the CV value of 0.4373 indicates low reliability and precision of the experimental data (Ifeanyi-nze FO and Akhiehiero ET, 2023). The high R^2 value of 0.9917% showed that the model satisfactorily represents the relationship between the independent variables like molar ratio, temperature, time and the response variable like COBL. The R^2 indicates that 99.17% variability is explained by the model, while only 0.83% remains unexplained. Furthermore, the regression model provided multiple correlation coefficients R^2 close to 1, suggesting excellent predictive capability (Mustapha AO, *et al*., 2020). The Predicted R^2 of 0.8713 is in reasonable agreement with the adjusted R^2 of 0.9811, with a difference of <0.2. Adequate Precision measures the signal to noise ratio with a desirable ratio >4. The obtained ratio of 31.22 in this study indicates an adequate signal, confirming that this model can effectively navigate the design space.

Model prediction

Table 10, showed the comparison between the actual values of COBL yield and the predicted values from the quadratic model. The regression coefficient R^2 represents that the accuracy and generalizability of the polynomial model. The predicted R^2 value 0.8713 is in reasonable agreement with the adjusted R^2 value of 0.9811, suggesting a strong correlation between the remarked values and the predicted data. Normal plot of residual was used to check the distribution of residuals. The alignment of residual points along the linear graph indicates that the residuals do not adversely affect the model's prediction.

Table 10: Statistical information for ANOVA of quadratic model

Parameter	Value
Standard deviation	0.3627
Mean	82.93
CV	0.4373
R^2	0.9917
Adjusted R^2	0.9811
Predicted R^2	0.8713
Adequate precision	31.2204

This signifies that the model is extremely accurate without any noise and

the results are reproducible. In the plot of actual value *vs.* predicted value, the close distribution of points between experimental and the predicted values along the straight lines indicate a good relationship between the experimental yield and the predicted yield of COBL. These plots further confirm that the selected model is adequate for predicting response variables in the experimental data (*Figure 2*).

Effect of process parameter on CAO biolubricant COBL yield

The relationship between the variables in linear, interactive and quadratic models affecting COBL yield has been statistically obtained using ANOVA (*Table 10*).

However, the effects of these variables and their interactions were not well established. A 3D response surface plots and 2D interaction plots can be used to examine the effect of the variables on the COBL yield.

One factor response on CAO biolubricant COBL yield

Effect of molar ratio on COBL: *Figure 3* shows the effect of molar ratio on the COBL yield. The response surface plot was present at varying molar ratio while, keeping the temperature 80°C and the reaction time at 90 minutes constant. The plot showed that high yields were obtained at both the lowest and highest molar ratios. The optimum yield was found to be 85.9642% at molar ratio of 3, closely followed by a yield of 85.6368% at molar ratio of 7. In contrast, a molar ratio of 5 showed lower COBL yield of around 82%. The ANOVA results showed linear effect of molar ratio is insignificant, the quadratic effect is significant for COBL yield (*Figure 3a*).

Effect of temperature on COBL: The relationship between temperature and COBL yield is small, as demonstrated by the ANOVA analysis, which shown an insignificant relationship p-value>0.05. When the molar ratio was fixed at 5 and the reaction time at 90 minutes, the yield varied within the range of 81.50%-82.65% (*Figure 3b*). This indicates that temperature does not significantly affect boilubricant yield. However, the maximum COBL yield was obtained at the temperature of 80°C with the value 82.65%.

Effect of contact time on COBL: The plot of COBL yield % obtained at different reaction time in fixed molar ratio percentage and temperature 140°C was showed in *Figure 3c*. The response surface plot shows that maximum yield was obtained in 90 minutes' reaction time and lowest yield was obtained at 60 minutes. This shown that 90 minutes is the optimum reaction time for COBL synthesis. The ANOVA for reaction time (C) showed a significant relationship with COBL yield. The response surface plot explains the relationship (*Figure 3d*).

Two factors interaction effect on CAO biolubricant COBL yield

Effect of molar ratio and temperatu re on COBL yield: *Figure 4* illustrates the interaction of molar ratio and temperature on the COBL yield. The molar ratio and temperature were varied from low to high while the reaction time constant at 90 minutes. (*Figure 4a*) showed the 3D response surface plot of the interaction while (*Figure 4b*) illustrated the 2D response. The response surface plots indicate that a high COBL yield was obtained at both high and low combinations of temperature and molar ratio as well as low temperature and molar ratio. In this study, that increasing in the molar ratio and temperature lead to decrease in COBL yield, however the trend changed at medium value molar ratio 5 and temperature 80°C, where the COBL yield increased. This indicated the interaction between the molar ratio and temperature is insignificant to the COBL yield. (Ocholi O, *et al.*, 2018) observed that for temperature, yield (Y) increased with an increasing mole ratio until it plateaued; whereas at lower temperature, the yield followed a parabolic path. At a fixed molar ratio, increasing temperature resulted in higher yields until a point where further increases had no significant effect. The area under the 3D plot showed that maximum yield was obtained at a molar ratio of 3 and at high temperature. These findings are consistent those who reported and noted that low temperature with high molar ratio yielded 84.52 wt %, while high temperature combined with low molar ratio resulted in an increase up to 93.08 wt %.

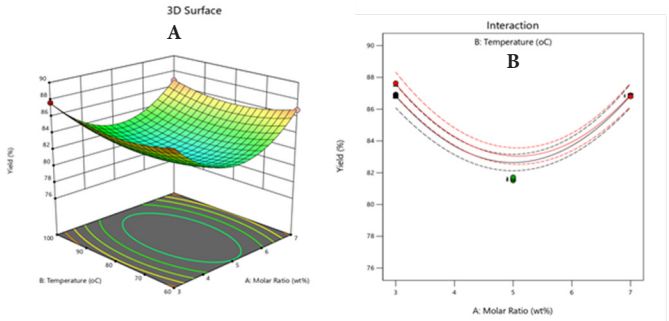

Figure 4: a): 3D response surface plot of temperature and molar ratio against COBL yield and b): 2D response surface plot of temperature and molar ratio against COBL yield

Effect of molar ratio and reaction time on COBL yield: *Figure 5*, shows the interaction of molar ratio and reaction time on the yield of COBL was analyzed using 3D and 2D response surface plots as showed in *Figure 5a*. These plots showed the effects of varying molar ratios and reaction times at a fixed temperature of 80°C. The highest COBL yield was achieved at a reaction time of 90 minutes and a molar ratio 3. The 3D plot shows that the COBL yield increases with reaction time until it reaches the optimum time of 90 minutes, after which the yield begins to decrease. Conversely, there is a decrease the COBL yield with an increase in molar ratio until it changes to an increase after reaching a molar ratio of 6. This may be due to the time to complete the stoichiometric ratio (2:1) between methyl ester and ethylene glycol in biolubricant synthesis. Overall, the results indicate that the interaction between molar ratio and reaction time is more statistically significant than interaction of molar ratio and temperature (*Figure 5b*).

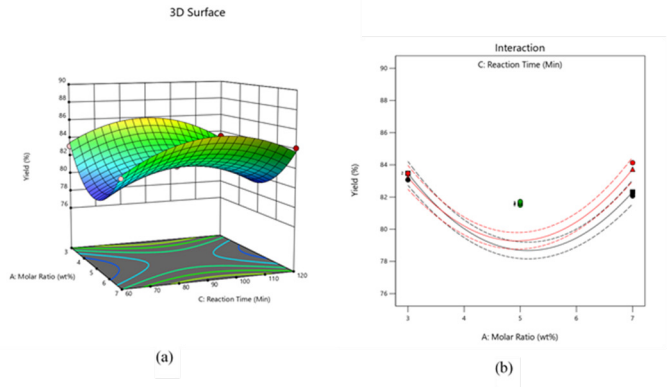

Figure 5: a): 3D response surface plot of molar ratio and reaction time against COBL yield and b): 2D response surface plot of molar ratio and reaction time against COBL yield

Effect of temperature and reaction time on COBL yield: *Figure 6*, illustrates the effect of temperature and reaction time on the yield of COBL at a fixed molar ratio of 3. The 3D and 2D response surface plots showed a good interaction between the two variables by a significant relationship was indicated by the ANOVA results (*Table 8*). The plot showed that at low reaction times, an increase in temperature leads to a higher COBL yield (*Figure 6a*). Similar effect is observed at high reaction times; however, the highest COBL yield occurs at a reaction time of 90 minutes for low and high temperature. At all temperatures, there is an increase in COBL yield with an increase in reaction time until the optimum reaction time of 90 minutes is reached, after which the yield begins to decrease. The results obtained in this study is related with the findings of (Ifeanyi-Nze FO and

Akhiehiero ET, 2023) who reported that an increase in reaction temperature accelerates the formation of biolubricant over a shorter time. This present study confirms that the optimum COBL yield occurs at a reaction time of 90 minutes, at high and low temperatures (*Figure 6b*).

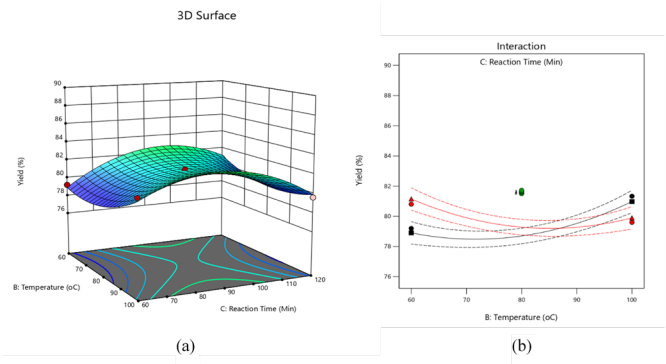

Figure 6: a): 3D response surface plot of temperature and reaction time against COBL yield and b): 2D response surface plot of temperature and reaction time against COBL yield

Interactions of all factors on CAO biolubricant COBL yield

The perturbation plot for the model illustrates the interaction of the three variables molar ratio, temperature and reaction time on the response yield. Perturbation analysis provides an outline of a reaction's characteristics. For response surface designs, the perturbation plot demonstrates how changes in response occur when any of the parameters deviate from a reference point, while all other components are held constant at their reference values (Ifeanyi-nze FO and Akhiehiero ET, 2023). The perturbation plot obtained for the three variables reaction time factor C, molar ratio factors A and temperature factor B. The analysis demonstrates that reaction time and molar ratio have a significant effect on the yield of COBL, while temperature has a lesser impact. This is due to the steeper slope of the factors showed on the perturbation plot. Specifically, factor C exhibits the steeper slope, closely followed by factor A, whereas factor B a much smaller slope. (Ifeanyi-nze FO and Akhiehiero ET, 2023) also reported that temperature and mole ratio have a more impact on biolubricant yield while time had the most negligible effect.

Process variable optimization and validation

Table 11, illustrates the optimization results predicted by the model. The result with the highest desirability was selected, revealing the ideal and optimum conditions for COBL synthesis a mole ratio of 3:1, a temperature of 80°C and a reaction time of 90 minutes. The optimum conditions were tested experimentally, yielding a value of 86.23%, which aligns closely with the predicted value of 85.96%, as shown in *Table 12*.

The results obtained in this study are related to some literature. (Ifeanyi-nze FO and Akhiehiero ET, 2023) reported the optimum conditions for *Jathropha* oil biolubricant synthesis to be a mole ratio of 3.87:1, a reaction time of 202.40 minutes and a reaction temperature of 128.95°C, which yielded a biolubricant with a yield of 94.12%. (Inegbenoise OO and Akhihiero ET, 2022) recorded optimum conditions for JBL synthesis is to be a temperature of 130°C, an Ethylene Glycol (EG) to FAME molar ratio of 3.5 and a reaction time of 180 minutes, resulting a yield of 88.74%. (Ocholi O, *et al*., 2018) investigated the operating process variables for *Jatropha* biolubricant production and found an optimum temperature of 150°C, a reaction time of 200 minutes and a *Jatropha* Methyl Ester (JME) to Trimethyl-ol-Propane (TMP) molar ratio of 5:1 and obtained a yield of 84.38% by (Inegbenoise OO and Akhihiero ET, 2022). (Borugadda VB and Goud VV, 2015) reported the optimum conditions for the epoxidation process of COBL, which included a substrate ratio of 1.65 mol, a catalyst loading of 15.14 wt% and a reaction time of 2.81 hours at a reaction temperature at 52.8°C. The response achieved was 3.85% by mass, which agrees with the predicted value from their model.

Properties of CAO biolubricant COBL

The properties of the COBL are presented in *Table 13*. Viscosity, viscosity index and pour point are important parameters in assessing the characteristics of lubricant. Viscosity is one of the most important characteristics of a lubricant, as it explains the flow resistance of the fluid at the various temperature. If a lubricant's viscosity is even slightly off from what is required for a component and application, it will not be able to sufficiently lubricate that component. This misalignment can lead to significant harm or even device failure. In this study, the kinematic viscosity of COBL was measured at two temperatures at 40°C and 100°C were 65.17 cSt and 10.5 cSt respectively. The synthesized ethylene glycol-based biolubricant has good viscosity, aligning with ISO VG 32 and ISO VG 46 standard specifications for light gear lubricant. It is crucial to choose one that maintains a stable viscosity across a wide temperature range. The lubricant's Viscosity Index (VI) is a key metric that indicates how temperature influences viscosity. This value is close to the findings of (Ifeanyi-nze FO and Akhiehiero ET, 2023), who reported the value of 40.08 cSt at 40°C and 9.21 cSt at 100°C for an ethylene glycol-based *Jatropha* biolubricant. Additionally, (Audu TO, *et al*., 2013) reported viscosities of 35.42 cSt at 40°C and 7.93 cSt at 100°C for sesame biolubricant. The relationship between kinematic viscosity and temperature of a substance is described by the term viscosity index. When the viscosity index is low, the oil will become very watery at high temperatures and rather thick at low temperatures. This indicates a strong dependence of viscosity on temperature. A high VI denotes minimal change in viscosity over a wide temperature range.

A higher VI indicates better quality lubricant. Oils with VI-values >130 can be used in a wide range of engines, providing enhanced performance. In this study, the VI of the COBL was determined from its kinematic viscosity at 40°C and 100°C to be 150. This value obtained is within the ISO VG 32 and ISO VG 46 lubricant standard. (Ifeanyi-nze FO and Akhiehiero ET, 2023) reported a higher VI of 205 for *jatropha* biolubricant, While, (Audu TO, *et al*., 2013) reported a VI of 206 for sesame biolubricant. A closer VI value was obtained by (Rao Z, *et al*., 2012) with a value of 180 for Trimethylolpropane (TMP) esters produced from *Jatropha curcas* and 162-172 for polyol esters of 10 undecenoic acid. Another important characteristic of biolubricant is the pour point, which is essential for evaluating flow qualities at low temperatures. The pour point is defined as the temperature at which lubricants stop to flowing determining their usability in low-temperature usability conditions. *Table 13*, shows COBL has a pour point of -10.8°C, which is closer to the ISO lubricant standard. This value is higher than those reported by (Ifeanyi-nze FO and Akhiehiero ET, 2023), who reported pour points of -15°C and -12°C, respectively. This indicates that COBL can operate at lower temperatures without clogging the filter. Additionally, a lubricant's flash point can be used to assess its flammability (Mustapha AO, *et al*., 2021). The flash point of the biolubricant made from CAO is 96°C, which represents a notable improvement over the equivalent biodiesel's flash point of 84°C. This increase in flash point can be attributed to the chemical alterations undergone by the base oil. The flash point of COBL is significantly lower than that of *Jatropha* biolubricant, which has a flash point of 215°C as reported by (Ifeanyi-nze FO and Akhiehiero ET, 2023).

The cloud point of COBL was determined to be 7.1°C. The cloud point refers to the temperature below which a biolubricant forms a cloudy appearance, indicating the onset of solidification. The obtained value of 7.1°C is significantly higher than the result reported by (Ifeanyi-nze FO and Akhiehiero ET, 2023), Which was 0.86°C. Overall, the synthesized COBL not only exhibits high quality with improved properties compared to its base oil but also meets the requirements for ISO VG 32 and ISO VG 46 lubricants.

Table 11: COBL actual yield *vs.* model's predicted yield

Run order	Actual value	Predicted value	Residual	Standard order
1	81.60	81.61	-0.0060	15
2	83.47	83.22	0.2450	7
3	84.13	83.73	0.4025	8
4	79.20	78.90	0.2963	9
5	81.33	80.98	0.3513	10
6	79.60	79.90	-0.2963	12
7	86.80	86.85	-0.0513	2
8	81.57	81.61	-0.0360	13
9	86.80	86.91	-0.1063	4
10	81.72	81.61	0.1140	17
11	81.50	81.61	-0.1060	14
12	86.93	86.82	0.1063	1
13	81.64	81.61	0.0340	16
14	87.64	87.59	0.0512	3
15	80.80	81.15	-0.3513	11
16	82.07	82.31	-0.2450	6
17	83.07	83.47	-0.4025	5

Table 12: Validation of optimum conditions

Solution 1 of 100 response	Predicted Mean	Predicted Median	Observed	Std. Dev.	n	SE Pred	95% PI low	Data Mean	95% PI high
Yield	85.9642	85.9642	-	0.362707	1	0.423374	84.9631	86.23	86.9654

Table 13: Properties of castor oil biolubricant and comparison with other plant based biolubricants and ISO viscosity grades

Physicochemical properties	Castor Oil Biolubricant (COBL)	[a]*Jatropha* biolubricant	[b]Sesame biolubricant	ISO standard VG 32	ISO standard VG 46	ISO standard VG 68
Kinematic viscosity (cSt, 40°C)	65.17	61.08	35.42	>28.8	>41.4	>61.4
Kinematic viscosity (cSt, 100°C)	10.5	9.21	7.93	>4.1	>4.1	>4.1
Viscosity index	150	205	206	>90	>90	>198
Pour point (°C)	-10.8	-15	-12	<-10	<-10	<-10
Flash point (°C)	96	215	-	-	-	-
Cloud point (°C)	7.1	0.86	-	-	-	-

Note: a: *Jatropha* biolubricant; b: Sesame biolubricant

CONCLUSION

The physicochemical properties of CAO, such as its high viscosity, iodine value and saponification value makes it a suitable non-edible vegetable oil for applications in bio-based lubricants. The esterification reaction effectively reduces the FFA content of CAO for biolubricant synthesis. The reduction in FFA contributes to a high yield of COME biodiesel produced. The ANOVA and model fittings indicated that the quadratic regression polynomial model is effective in the optimization of the COBL yield using RSM. The Optimization process, employing a BBD within RSM, identified the optimum conditions for COBL synthesis as a mole ratio of 3:1, a temperature of 80oC and a reaction time of 90 minutes. The optimum conditions were experimented and the value obtained was 86.23% which aligns with the predicted value of 85.96%. A Comparative analysis of the properties of the synthesized and optimized CAO biolubricant demonstrated that it meets the requirements for ISO VG 32 and ISO VG 46 biolubricants, which indicated the optimized CAO biolubricant is an acceptable replacement for petroleum-based lubricants in automobiles and biolubricant pilot plant.

REFERENCES

1. Attia NK, El-Mekkawi SA, Elardy OA, Abdelkader EA. Chemical and rheological assessment of produced biolubricants from different vegetable oils. J Fuels. 2020; 271: 117578.
2. Africa automotive lubricants market size & share analysis - growth trends & forecasts up to 2026. 2023.
3. Benedicto E, Carou D, Rubio EM. Technical, economic and environmental review of the lubrication/cooling systems used in machining processes. Procedia Eng. 2017; 184: 99-116.
4. Rakkan T, Paichid N, Yunu T, Klomklao S, Sangkharak K. Synthesis and characterization of biolubricant from POME oil and hepatopancreas lipase from pacific white shrimp *Litopenaeus vannamei*. Chiang Mai J Sci. 2018; 45: 2438-2453.
5. Mustapha AO, Ayoku HB, Amao HA. New alkyd resins from underutilized indigenous seed oils: Synthesis and characterization. Karbala Int J Mod Sci. 2023; 9(2): 216-225.
6. Heikal EK, Elmelawy MS, Khalil SA, Elbasuny NM. Manufacturing of environment friendly biolubricants from vegetable oils. Egypt J Pet. 2017; 26(1): 53-59.
7. Patel VR, Dumancas GG, Viswanath LC, Maples R, Subong BJ. Castor oil: Properties, uses, and optimization of processing parameters in commercial production. Lipid Insights. 2016; 9: 1-12. [Pubmed]
8. Yeboah A, Ying S, Lu J, Xie Y, Amoanimaa-Dede H, Boateng KG, *et al*. Castor oil *Ricinus communis*: A review on the chemical composition and physicochemical properties. J Food Sci Technol. 2020; 41: 399-413.
9. Musa U, Mohammed IA, Sadiq MM, Aberuagba F, Olurinde AO, Obamina R. Synthesis and characterization of trimethylolpropane-based biolubricants from castor oil. Niger J Chem Eng. 2015; 5-7.
10. Uppar R, Dinesha P, Kumar S. A critical review on vegetable oil-based bio-lubricants: Preparation, characterization, and challenges. J Environ Dev Sustain. 2023; 25(9): 9011-9046.
11. Bekele BA, Ourgessa AW, Terefe AA, Hailu SS. Studies on ethiopian castor seed *Ricinus communis* L: Extraction and characterization of seed oil. J Nat Prod Resour. 2018; 4(2): 188-190.
12. Mustapha AO, Adepoju RA, Ajiboye RY, Afolabi YT, Jimoh AA, Abdulsalam ZA. Production, properties and fatty acids profile of some refined vegetable oils based biodiesels. Asian J Adv Res. 2021; 346-355.
13. Mustapha AO, Babatunde A, Akinola O, Olododo H, Afolabi Y, Abdulfatai T. Trimethylolpropane based biolubricant synthesis from sweet almond *Prunusamygdalus dulcis* seed oil for use in automotive applications. J Turk Chem Soc A: Chem. 2023; 10(2): 371-380.
14. Ocholi O, Menkiti MC, Aniagor CO. Optimization of biodegradable lubricant basestock synthesis from *Jatropha curcas* seed oil using response surface methodology. J Appl Eng Sci. 2021; 19(1):409-426.
15. Betiku E, Odude VO, Ishola NB, Bamimore A, Osunleke AS, Okeleye AA. Predictive capability evaluation of RSM, ANFIS and ANN: A case of reduction of high free fatty acid of palm kernel oil *via* esterification process. Energy Convers Manag. 2016; 124: 219-230.
16. Leevijit T, Prateepchaikul G, Maliwan K, Mompiboon P, Okaew S, Eiadtrong S. Production, properties, and utilization of degummed/esterified mixed crude palm oil-diesel blends in an automotive engine without preheating. J Fuels. 2016; 182: 509-156.
17. Reshad AS, Tiwari P, Goud VV. Extraction of oil from rubber seeds for biodiesel application: Optimization of parameters. Fuel. 2015; 150: 636-644.
18. Pradhan S, Saha C, Kumar M, Naik SN. Transesterification and reactive extraction of castor oil for synthesis of biodiesel/biolubricant. IOP Conf Ser Earth Environ Sci. 2021; 785(1).
19. Mokhtar SM. Synthesis of ethylene glycol diesters as bio-lubricant oil from *Jatropha* methyl esters. Doctoral dissertation, university of Gezira. 2018.
20. Guo S, Li C, Zhang Y, Yang M, Jia D, Zhang X, *et al*. Analysis of volume ratio of castor/soybean oil mixture on minimum quantity lubrication grinding performance and microstructure evaluation by fractal dimension. Ind Crop Prod. 2018; 111: 494-505.
21. Yusuf AK, Mamza PA, Ahmed AS, Agunwa U. Extraction and characterization of castor seed oil from wild *Ricinus communis* Linn. Int J Sci Environ Technol. 2015; 4(5): 1392-1404.
22. Silitonga AS, Shamsuddin AH, Mahlia TM, Milano J, Kusumo F, Siswantoro J. Biodiesel synthesis from *Ceiba pentandra* oil by microwave irradiation-assisted transesterification: ELM modeling and optimization. J Renew Energy. 2020; 146: 1278-1291.
23. Singh D, Sharma D, Soni SL, Sharma S, Kumari D. Chemical compositions, properties, and standards for different generation biodiesels: A review. J Fuels. 2019; 253: 60-71.
24. Binhweel F, Bahadi M, Pyar H, Alsaedi A, Hossain S, Ahmad MI. A comparative review of some physicochemical properties of biodiesels synthesized from different generations of vegetative oils. J Phys Conf Ser. 2021; 1900(1): 012009.
25. Sivaramakrishnan K, Ravikumar P. Determination of higher heating value of biodiesels. Int J Eng Sci Tech. 2011; 3(11): 7981-7987.
26. Mohammed IS, Aliyu M, Dauda SM, Balami AA, Yunusa BK. Synthesis and optimization process of ethylene glycol-based bio-lubricant from Palm Kernel Oil (PKO). 2019.
27. Ifeanyi-Nze FO, Akhiehiero ET. Optimization of the process variables on biodegradable industrial lubricant basestock synthesis from *Jatropha curcas* seed oil *via* response surface methodology. Front Energy Res. 2023; 11: 1169565.
28. Mustapha AO, Adepoju RA, Afolabi YT. Optimization of vegetable oil-based biodiesels by Multi-Response Surface Methodology (MRS) using desirability functions. J Chem Soc Niger. 2020; 45(5).
29. Ocholi O, Menkiti M, Auta M, Ezemagu I. Optimization of the operating parameters for the extractive synthesis of biolubricant from sesame seed oil *via* response surface methodology. Egypt J Pet. 2018; 27(3): 265-275.

30. Inegbenoise OO, Akhihiero ET. Effects of process variables on biolubricant production from *Jatropha curcas* seed oil. J Eng Dev. 2022; 14(1).

31. Borugadda VB, Goud VV. Response surface methodology for optimization of bio-lubricant basestock synthesis from high free fatty acids castor oil. J Energy Sci Eng. 2015; 3(4): 371-383.

32. Audu TO, Aluyor EO, Egualeona S, Momoh SS. Extraction and characterization of Chrysophyllumalbidum and Luffa cylindrica seed oils. J Petrol Tech Dev. 2013; 3(1): 1-7.

33. Rao Z, Gao J, Zhang B, Yang B, Zhang J. Cisplatin sensitivity and mechanisms of anti-HPV16 E6-ribozyme on cervical carcinoma CaSKi cell line. Chin J Clin Oncol. 2012; 11: 237-242.